Oliver, S., Pavier, M., & Mostafavi, M. (2016). Applying fracture mechanics to cracked components subjected to unloading. In ASME 2016 Pressure Vessels and Piping Conference: Volume 5: High-Pressure Technology; Rudy Scavuzzo Student Paper Symposium and 24th Annual Student Paper Competition; ASME Nondestructive Evaluation, Diagnosis and Prognosis Division (NDPD); Electric Power Research Institute (EPRI) Creep Fatigue Workshop. (Vol. 5). [V005T09A016] American Society of Mechanical Engineers (ASME). DOI: 10.1115/PVP2016-63575

Proceedings of the ASME 2016 Pressure Vessels and Piping Conference
PVP2016
July 17-21, 2016, Vancouver, British Columbia, Canada

PVP2016-63575

APPLYING FRACTURE MECHANICS TO CRACKED COMPONENTS SUBJECTED TO UNLOADING

Sam Oliver, Martyn Pavier and Mahmoud Mostafavi
Department of Mechanical Engineering
University of Bristol
Bristol, UK

ABSTRACT

The *J*-integral is widely used as a fracture parameter for elastic-plastic materials. The *J*-integral describes the intensity of the stress field close to the crack tip in a power-law hardening material under a set of well-known restrictions. This study investigates what happens when one of these restrictions is broken, namely the requirement for no unloading to occur.

In this work, a centre-cracked plate is subjected to a single cycle of load in which unloading occurs. A remote tensile stress is applied, then released, then applied again up to and beyond its initial magnitude. The *J*-integral at each step of the analysis is calculated using finite element analysis. Its validity as a fracture parameter at each step is discussed with the aid of results from a strip yield analysis of the same problem. The relevance of the results in the context of structural integrity assessment is discussed.

INTRODUCTION

The *J*-integral [1] describes the intensity of the stresses near to the tip of a crack in a power-law hardening elastic plastic material under certain conditions. One requirement is that loading is monotonic (no unloading occurs). The stress field near to the tip of a crack in a power-law hardening material was calculated by Hutchinson, Rice and Rosengren, otherwise known as the HRR field [2-4]:

$$\sigma_{ij}^{HRR} = \sigma_0 \left(\frac{EJ}{\alpha \sigma_0^2 I_n r} \right)^{\frac{1}{n+1}} \tilde{\sigma}_{ij}(n,\theta) \qquad (1)$$

where: E is Young's modulus; J is the J-integral; σ_0, α and n are parameters which describe the shape of the stress-strain curve of the material; $I_n(n)$ is an integration constant; $\tilde{\sigma}_{ij}(n,\theta)$ is a dimensionless stress function; and $(r;\theta)$ are polar co-ordinates with origin at the crack tip.

One method of assessing the integrity of a structure containing a defect is to make an FE model and calculate the *J*-integral. This can then be compared with a critical value of *J* which is determined in fracture toughness tests. It is straightforward to calculate the *J*-integral in an FE model as long as there is sufficient stress and displacement information to do so. However, neither being able to calculate the *J*-integral nor its contour independence are guarantors of its validity as a fracture parameter.

If any unloading occurs, then Equation (1) is no longer valid and the *J*-integral loses its meaning as an elastic plastic stress intensity factor. In components such as pressure vessels, it is unlikely that load is always applied monotonically through the entirety of their service lives. This study investigates the use of the *J*-integral as a stress intensity parameter under non-

monotonic conditions. A non-monotonic load sequence is applied to a centre-cracked plate model. Near tip stresses and the *J*-integral are calculated at different points in the sequence, both using FEA and a modified strip yield model. Near tip stresses are compared with the HRR field at every point. The interpretation of the results in terms of structural integrity assessment is discussed.

CENTRE CRACKED PLATE MODEL

A simple two dimensional geometry has been studied. The model is an infinite centre cracked plate (CCP) with a half crack length, *a*, of 0.1 m (Fig. 1). A remote tensile stress is applied to the cracked plate. This is then released. The load is then increased incrementally up to and beyond the original load. This loading sequence is illustrated in Fig. 2.

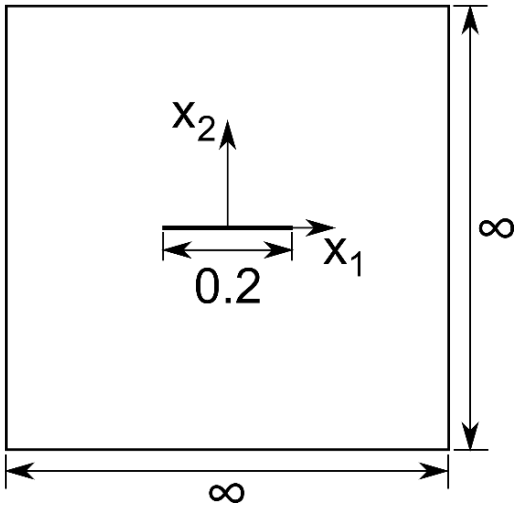

Fig. 1 – Infinite centre cracked plate containing a through crack with half-length, *a*, of 0.1 m.

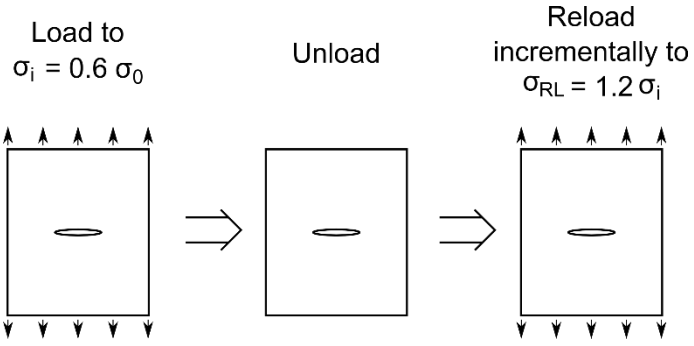

Fig. 2 – The non-monotonic loading sequence. An initial remote stress, σ_i, is applied, followed by unloading. The plate is then reloaded using an additional remote applied stress, σ_{RL}.

FINITE ELEMENT ANALYSIS

The finite element (FE) model is shown in Fig. 3. This is a quarter model, with two lines of symmetry. The infinite plate is represented by making the side length large compared to the crack. The crack exists due to the absence of the symmetry boundary condition along the crack face. The mesh in the vicinity of the crack tip is shown in Fig. 4. The smallest element is at the tip of the crack, with a side length of 10^{-4} m. The model was implemented in Abaqus 6.14 [5]. Quadratic plane stress elements (CPS8R) were used. Small strain assumptions were made so that the effects of crack tip blunting were not included in the analysis. Convergence studies were performed to confirm sufficient mesh refinement near to the crack tip.

Two different material models were used: elastic perfectly plastic, and power-law isotropic hardening. For the latter material, the Ramberg-Osgood equation describes the monotonic, uniaxial stress-strain behavior:

$$\frac{\varepsilon}{\varepsilon_0} = \frac{\sigma}{\sigma_0} + \alpha\left(\frac{\sigma}{\sigma_0}\right)^n \qquad (2)$$

The reference stress, σ_0, was defined at the yield point of the material, and the reference strain, ε_0, is σ_0/E. The hardening exponent, n, and offset term, α, define the shape of the curve. The values for these terms which were used in the model are given in Table 1. The elastic perfectly plastic material used these same values of E, ν and σ_0.

Equation (2) was discretised and input into Abaqus as an incremental plasticity material. The Ramberg-Osgood relation was chosen so that, under monotonic and proportional loading, the near crack tip stress fields agree with those calculated by Hutchinson, Rice and Rosengren (HRR) [2-4]. For calculation of the HRR field, $I_n(n)$ and $\tilde{\sigma}_{ij}(n,\theta)$ were evaluated using a program written by Galkiewicz and Graba [6]. The HRR solution for the elastic perfectly plastic model, which represents the limit where n is infinity, has been previously calculated by Shih [7].

The *J*-integral was calculated using the standard Abaqus formulation which does not account for residual stress. This is simply a domain integral interpretation of the contour integral formulation given by Rice [1]. Abaqus also includes a formulation which allows the definition of a residual stress field, but it was not used here for reasons discussed in the 'results and discussion' section of this paper. The *J*-integral was calculated using 30 different domain sizes to check for convergence. The value of *J* used for analysis was calculated using the largest domain, which is a square of side length approximately 10 times the half crack length.

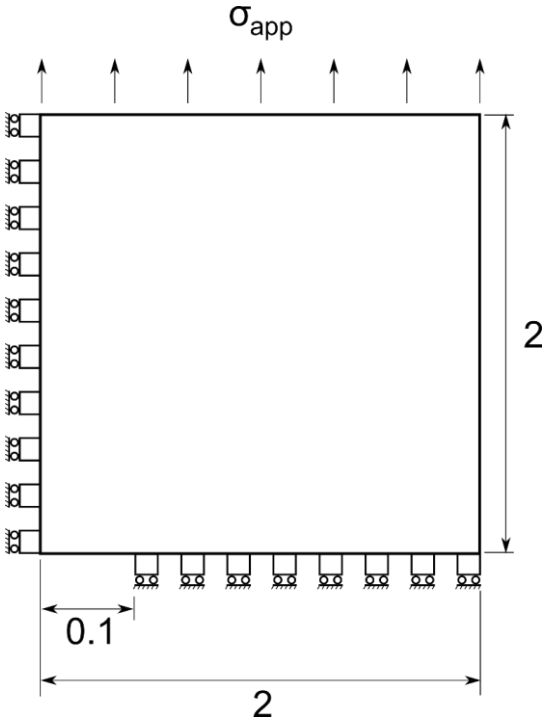

Fig. 3 – Quarter model of the centre cracked plate. Dimensions are in metres.

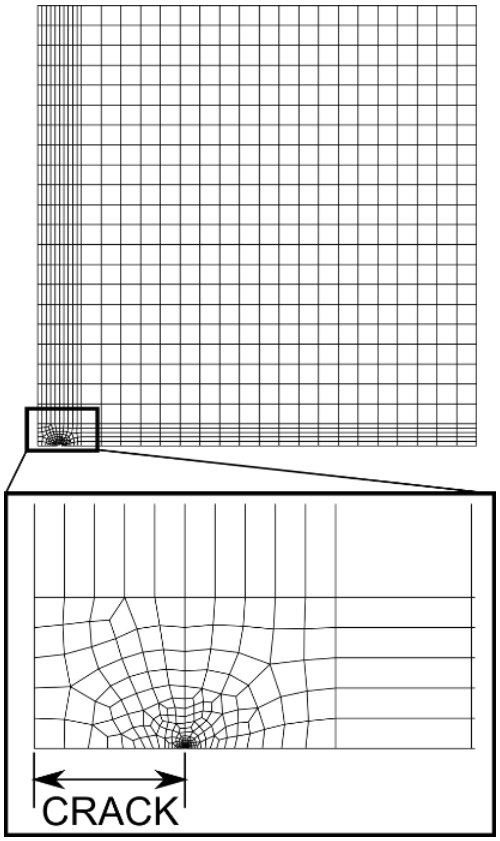

Fig. 4 – FE mesh of the centre cracked plate.

Table 1 – Properties of the Ramberg-Osgood material.

Young's modulus, E (GPa)	210
Poisson's ratio, ν	0.3
Ramberg-Osgood exponent, n	7
Ramberg-Osgood yield offset, α	0.84
Yield stress, σ_0 (MPa)	500

STRIP YIELD ANALYSIS

The standard strip yield model [8, 9] is shown in Fig. 5. The crack and its plastic zone are modelled as the superposition of two elastic solutions for a crack which extends all the way to the edge of the plastic zone. The first is that due to applied load. For a finite centre crack in an infinite plate:

$$K_{app} = \sigma_{app}\sqrt{\pi(a + r_p)} \tag{3}$$

where K_{app} is the stress intensity factor (SIF) due to remote applied load, σ_{app}, and r_p is the plastic zone size. The second solution is due to closure stresses equal to the yield stress acting over the plastic zone:

$$K_{sy} = 2\sigma_0\sqrt{\frac{a + r_p}{\pi}}\sin^{-1}\left(\frac{a}{a + r_p}\right) - \sigma_0\sqrt{\pi(a + r_p)} \tag{4}$$

The plastic zone size is adjusted until the sum of the SIF due to applied load and the SIF due to closure stresses is equal to zero at the edge of the plastic zone.

The basic strip yield analysis has been extended to account for combined residual stress and applied load. In this extended analysis, there now exists exists an additional contribution to the total SIF due to a non-uniform normal residual stress distribution, σ_{22}^{RS}:

$$K_{RS} = \frac{2}{\sqrt{\pi(a + r_{p)}}}\int_0^{a+r_p}\frac{\sigma_{22}^{RS}(x_1)}{\sqrt{1 - \left(\frac{x_1}{a + r_p}\right)^2}}dx_1 \tag{5}$$

The following can then be solved for the plastic zone size:

$$K_{app} + K_{sy} + K_{RS} = 0 \quad (6)$$

In the same manner as above, stress functions found using different elastic solutions can be added together. For simplicity, only the solutions for normal stress acting on the symmetry plane ($x_2 = 0$) are shown in the following analysis. The standard strip yield model superimposes two stress solutions. The first is due to the applied stress:

$$\sigma_{22}^{app} = \sigma_{app} \frac{x_1}{\sqrt{x_1^2 - \left(c + r_p\right)^2}} \quad (7)$$

The second is due to closure stress:

$$\sigma_{22}^{cl} = -\frac{2\sigma_0}{\pi} \int_a^{a+r_p} \frac{\sqrt{\left(a + r_p\right)^2 - \bar{x}_1^2}}{(x_1^2 - \bar{x}_1^2)\sqrt{1 - \left(\frac{a + r_p}{x_1}\right)^2}} d\bar{x}_1 \quad (8)$$

Two further solutions need to be accounted for when residual stress is present: one is the residual stress field itself, and the other is the stress field caused by introducing a crack into the residual stress field. The latter can be expressed as follows:

$$\sigma_{22}^{RD} = \frac{2}{\pi} \int_0^{a+r_p} \frac{\sigma_{22}^{RS}(\bar{x}_1)\sqrt{\left(a + r_p\right)^2 - \bar{x}_1^2}}{(x_1^2 - \bar{x}_1^2)\sqrt{1 - \left(\frac{a + r_p}{x_1}\right)^2}} d\bar{x}_1 \quad (9)$$

The total stress field can then be calculated:

$$\sigma_{22}^{total} = \begin{cases} 0, & 0 \le x_1 < a \\ \sigma_0, & a \le x_1 \le a + r_p \\ \sigma_{22}^{app} + \sigma_{22}^{cl} + \sigma_{22}^{RS} + \sigma_{22}^{RD}, & a + r_p < x_1 \end{cases} \quad (10)$$

The above procedure describes the modifications to the strip yield model required to account for residual stress. The stress and SIF results given above are known LEFM solutions [10], with the actual crack length replaced with $a+r_p$. This procedure can be used to model the load-unload-reload case in Fig. 2 by choosing σ_{22}^{RS} to be the stress field present after unloading. The strip yield solution for an unloaded crack calculated by Becker [11] was used for this purpose.

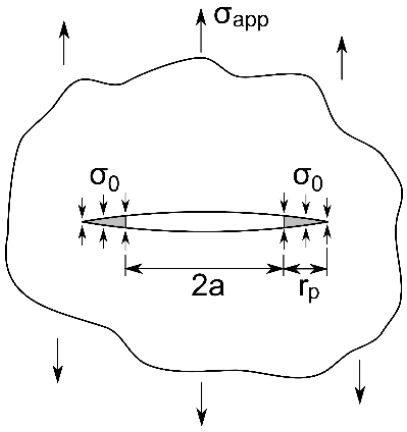

Fig. 5 – The standard strip yield model.

RESULTS AND DISCUSSION

The near-tip stress distributions for the elastic perfectly plastic CCP, calculated using FEA and the strip yield model, are shown in Fig. 6. The normal stress normalised by the yield stress is plotted against the distance ahead of the crack tip, *r*, on the symmetry plane ($x_2=0$) normalised by the crack length. The reloaded strip yield model works well when the applied reload is smaller than the initial applied load. Some disparity exists because the von Mises yield criterion permits stresses greater than the uniaxial yield stress in the FE model, whereas the strip yield model does not.

The near-tip stress distributions calculated using FEA at different points during the load cycle are shown in Fig. 7. The normal stress at each point, *r*, is normalised by the HRR field calculated at the same point. *J*-dominance is perfect when this is equal to one. On the x-axis, the distance ahead of the crack tip is normalised by the plastic zone size, defined as the region over which the equivalent plastic strains are greater than 0.2%. Results are shown for a strain hardening material, with $n=7$, and for an elastic perfectly plastic (EPP) material.

After unloading, the near tip stress is not characterised by HRR and the *J*-integral loses its meaning as a crack tip stress intensity parameter. This is to be expected, since the load is not monotonic. Fig. 7 (h) shows that *J*-dominance is once again achieved when the load is reapplied to just beyond the original load. The stress after unloading the EPP material is shown in Fig. 6 (b). This could be interpreted as a residual stress field which extends approximately as far as the plastic zone ahead of the crack tip. The contribution of this residual stress to the total stress diminishes as the magnitude of applied re-load is increased. For the strain hardening material, the residual stress is effectively wiped out when the amount of re-load is 1.2 times the original load. For the elastic perfectly plastic material, this occurs when the amount of re-load is equal to the original applied load. Assuming constant yield strength in the elastic perfectly plastic

analysis of warm pre-stress by Chell et al [12] gives the analogous result that previous loading is irrelevant if the magnitude of the final applied load is larger than the initial load.

This is a useful result for structural integrity assessment. For example, it may be necessary to assess the integrity of a cracked pressure vessel which has previously been subjected to an overload. The *J*-integral could be calculated with an FE model of the cracked vessel. The validity of *J* could be checked by plotting graphs similar to those in Fig. 7. If non-monotonic loading formed part of the analysis, *J*-dominance is unlikely to be achieved, and the analysis is not valid. If, however, an imaginary additional load were applied to the model of such a magnitude that *J* becomes valid again, and if such a value of *J* were acceptable, then the vessel is safe.

The *J*-integral appeared to have converged with increasing domain size at every analysis stage, excepting when evaluated immediately after the unload step in the strain hardening material. The lack of *J*-dominance in Fig. 7 (c-d) demonstrates that simply verifying the domain-independence of the *J*-integral is not sufficient in demonstrating its validity.

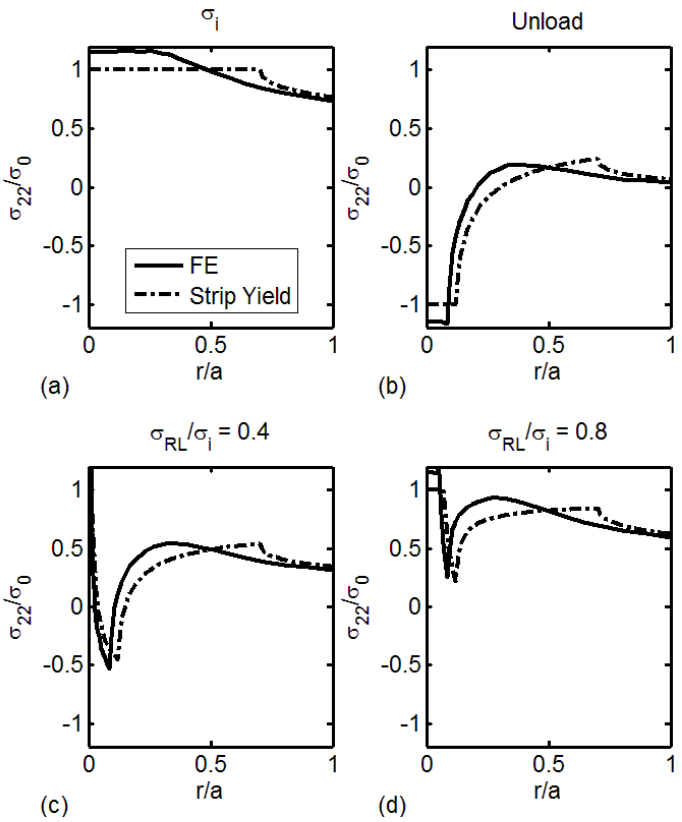

Fig. 6 – Near-tip stress fields calculated using FEA and the modified strip yield method at different points during the load cycle: after the initial load is applied (a); after unloading (b); after the plate has been reloaded to 0.4 times the initial load (c); and after the plate has been reloaded to 0.8 times the initial load.

Work has previously been carried out to modify the *J*-integral so that it is path-independent under complex load conditions including residual stress [13-15]. There is one such formulation available in Abaqus v6.14 which accounts for residual stress [5]. It may be tempting to treat the stress due to the initial load-unload cycle, such as that shown in Fig. 6 (b), as a residual stress field in one of these modified *J* formulations. However, even if a different value of *J* were calculated this would not improve *J* dominance, for example in Fig. 7 (b-f), since the near-tip stress fields are unchanged by the specifics of the *J* calculation.

If the *J*-integral characterises the near-tip stresses for a uniform residual stress field, but not for the near-tip residual stress field generated by unloading, it follows that there is a limiting size of residual stress field below which the *J*-integral is unable to characterise near-tip stresses. Future investigations could focus on defining this limiting size.

CONCLUSIONS

A centre cracked plate model has been investigated which is subjected to an initial load-unload cycle and then reloaded. The *J*-integral fails as a stress intensity parameter after unloading has occurred. *J* can become valid again simply by applying additional load. A modified strip yield model was developed to solve the problem assuming elastic perfectly plastic material properties. The model agrees well with FE results, and provides an additional useful tool for solving non-monotonic elastic plastic fracture problems.

ACKNOWLEDGMENTS

The authors would like to thank Amec Foster Wheeler for sponsoring a PhD studentship undertaken by Sam Oliver. Thanks are owed to the late Prof. David Smith for valuable technical guidance.

REFERENCES

1. Rice, J.R., *A path independent integral and the approximate analysis of strain concentration by notches and cracks.* Journal of Applied Mechanics, 1968. **35**: p. 379-386.
2. Hutchinson, J.W., *Singular Behaviour at End of a Tensile Crack in a Hardening Material.* Journal of the Mechanics and Physics of Solids, 1968. **16**(1): p. 13-31.
3. Hutchinson, J.W., *Plastic Stress and Strain Fields at a Crack Tip.* Journal of the Mechanics and Physics of Solids, 1968. **16**(5): p. 337-347.
4. Rice, J.R. and G.F. Rosengren, *Plane Strain Deformation near a Crack Tip in a Power-Law Hardening Material.* Journal of the Mechanics and Physics of Solids, 1968. **16**(1): p. 1-12.
5. *Abaqus v6.14.* Providence, RI, USA: Dassault Systemes Simulia Corp. .

6. Gałkiewicz, J. and M. Graba, *Algorithm for determination of σ˜ij(n,θ), ε˜ij(n,θ), u˜i(n,θ), dn(n), In(n) functions in Hutchinson-Rice-Rosengren solution and its 3d generalization.* Journal of theoretical and applied mechanics, 2006. **44**(1).
7. Shih, C.F., *Tables of Hutchinson-Rice-Rosengren singular field quantities.* Brown Univeristy Report, MRL E-147, 1983.
8. Dugdale, D.S., *Yielding of Steel Sheets Containing Slits.* Journal of the Mechanics and Physics of Solids, 1960. **8**(2): p. 100-104.
9. Rice, J.R., *Mathematical analysis in the mechanics of fracture*, in *Fracture - an advanced treatise*, H. Liebowitz, Editor. 1968, Academic Press.
10. Tada, H., P.C. Paris, and G.R. Irwin, *The Stress Analysis Of Cracks Handbook*. 3 ed. 2000, New York: ASME Press.
11. Becker, W., *Closed-form modeling of the unloaded mode I Dugdale crack.* Engineering Fracture Mechanics, 1997. **57**(4): p. 355-364.
12. Chell, G.G., J.R. Haigh, and V. Vitek, *A Theory of Warm Prestressing - Experimental Validation and the Implications for Elastic Plastic Failure Criteria.* International Journal of Fracture, 1981. **17**(1): p. 61-81.
13. Lei, Y., N.P. O'Dowd, and G.A. Webster, *Fracture mechanics analysis of a crack in a residual stress field.* International Journal of Fracture, 2000. **106**(3): p. 195-216.
14. Lei, Y., *J-integral evaluation for cases involving non-proportional stressing.* Engineering Fracture Mechanics, 2005. **72**(4): p. 577-596.
15. Beardsmore, D.W., *Jedi: A Code for the Calculation of J for Cracks Inserted in Initial Strain Fields and the Role of J and Q in the Prediction of Crack Extension and Fracture.* PVP2008-61169, 2008 ASME Pressure Vessels and Piping Conference, Chicago, Illinois, USA, 2009: p. 955-966.

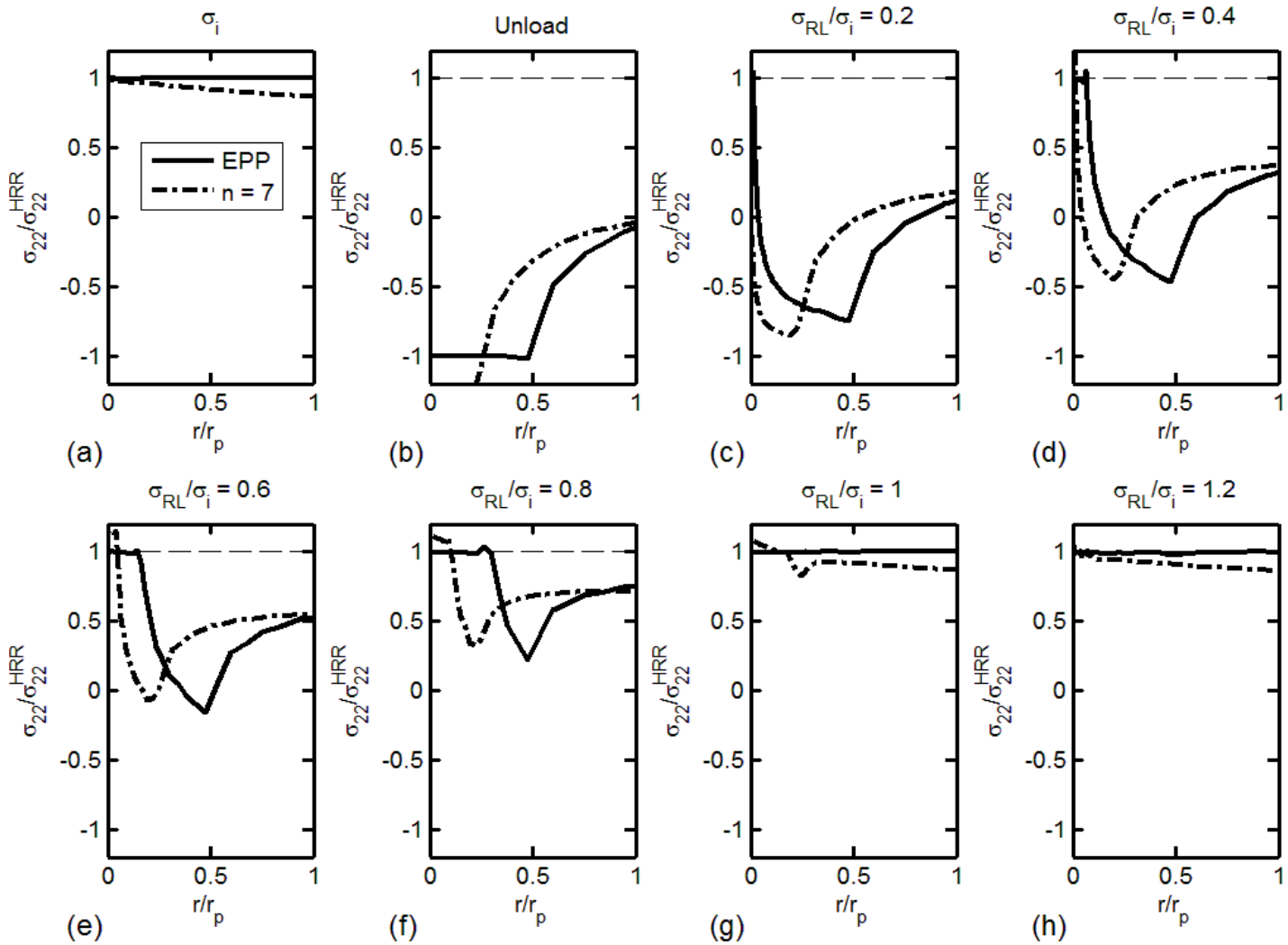

Fig. 7 – Near tip stress fields calculated using FEA at different points during the load cycle: after the initial load is applied (a); after unloading (b); and after the plate has been reloaded with increasing magnitude up to 1.2 times the initial load (c-h).